Comparison of carrier removal methods in the analysis of TV holography fringes by the Fourier transform method

Antonio Fernández, MEMBER SPIE

Universidade de Vigo

Departamento de Física Aplicada

ETSEIM Lagoas-Marcosende 9

36200 Vigo, Spain

Phone: + 34 986 812 216

Fax: + 34 986 812 201

E-mail: antfdez@uvigo.es

Guillermo H. Kaufmann, MEMBER SPIE

Consejo Nacional de Investigaciones Científicas y Técnicas y Universidad Nacional de Rosario

Instituto de Física de Rosario

Bv. 27 de Febrero 210 Bis

2000 Rosario, Argentina

Phone: + 54 41 85 3200

Fax: + 54 41 82 1772

E-mail: guille@ifir.ifir.edu.ar

Ángel F. Doval

Universidade de Vigo

Departamento de Física Aplicada

ETSEIM Lagoas-Marcosende 9

36200 Vigo, Spain

Phone: + 34 986 812 216

Fax: + 34 986 812 201

E-mail: adoval@uvigo.es

Jesús Blanco-García

Universidade de Vigo

Departamento de Física Aplicada

ETSEIM Lagoas-Marcosende 9

36200 Vigo, Spain

Phone: + 34 986 812 216

Fax: + 34 986 812 201

E-mail: jblanco@uvigo.es

José L. Fernández

Universidade de Vigo

Departamento de Física Aplicada

ETSEIM Lagoas-Marcosende 9

36200 Vigo, Spain

Phone: + 34 986 812 216

Fax: + 34 986 812 201

E-mail: jlfdez@uvigo.es

Abstract. Carrier removal is a key step in the Fourier transform method (FTM) of fringe pattern analysis because it can give raise to significant errors in the recovered phase. In this paper, the existing methods of fringe carrier removal in FTM are reviewed and a comparison of three different methods, translation of the sidelobe to the frequency origin, least-squares fit and subtraction of the phase of the undeformed carrier fringes, is presented. Computer-generated fringe patterns are used in order to determine the differences between the original and the retrieved phase distributions. Several figures of merit are proposed to assess the performance of the mentioned methods. Experimental fringe patterns, obtained by double-pulsed-subtraction TV holography, are analized by the methods considered here, and the retrieved phase distributions are also compared.

Subject terms: Fourier transform method; fringe analysis; TV holography; ESPI; speckle metrology

1. Introduction

The Fourier transform method (FTM) of fringe pattern analysis was first demonstrated by Takeda *et al.*[1] in 1982. Since then, it has become one of the most popular phase evaluation methods used in high accuracy measurement systems. FTM advantages temporal phase measurement methods mainly in that all the information needed to reduce an interferogram to a phase map is recorded simultaneously.[2] This means that fast temporal phase variations can be measured. The influence of several error sources in FTM has been extensively studied and different solutions for each particular error source have been proposed.[2-9] Removal of the phase due to spatial carrier is a key step in fringe analysis by FTM, because it can give raise to significant errors in the retrieved phase. However, phase errors associated to the existing methods of carrier removal have not been quantified. In this paper, three different methods of fringe carrier removal in FTM are compared. Computer-generated fringe patterns are analized by these three methods in order to accurately determine the differences between the original and the retrieved phase distributions. Several parameters are used to assess quantitatively the performance of each method. In addition, experimental fringe patterns obtained by double-pulsed subtraction TV holography are also analyzed by the three aforementioned methods, and the retrieved phase distributions are also compared.

2. Carrier removal in Fourier transform fringe analysis

In this section, a brief review of the fringe carrier removal methods which have appeared in the literature is presented. These methods can be classified according to the domain in which carrier is removed,[11] either the Fourier or the spatial domains.

Takeda *et al.*[1] have removed the carrier phase in the Fourier plane by translating the sidelobe to the frequency origin (TSFO), and then computing the inverse Fourier transform. A major drawback due to the digitization of the data arises in applying this method, because the translation is constrained to integer values of the spatial frequency. Nugent has proposed a refinement of this method based on library minimization routines to correct the errors in the retrieved phase when the value of the carrier frequency is non integer.[3] A requirement for this improvement to be successfully implemented is that the phase object is only of limited spatial extent, i. e., the interferogram has areas devoid of modulation, which is not true in most applications.

A variety of approaches has been proposed for carrier removal in the spatial domain. Bone *et al.*[4] have estimated the carrier phase by least-squares fit (LSF) of a plane to the retrieved phase distribution in a region that has no contribution from the desired information. Then, heterodyning is removed by direct subtraction of the calculated plane in the spatial domain. If carrier fringes are undesirably twisted, a simple linear fit will introduce errors. For the same case, Gu and Chen have proposed a bilinear surface or some other function to describe the carrier.[10] Obviously, the accuracy of the retrieved phase is dramatically affected by the right choice between a particular surface or another. Furthermore, the requirement of an information-free region in the interferograms cannot always be fulfilled. A similar approach has been suggested for the cases in which the carrier frequency can be measured or calculated (for example, by measuring the tilt angle of the mirror in the interferometer). However, generally it is not possible or extremely difficult to obtain a reliable estimation for the carrier frequency,[11] and therefore this method will not be considered here. Finally, the

true distribution of the carrier phase can be obtained by analyzing a fringe pattern recorded previous to the event (deformation, change of refraction index, etc.) that gives raise to the phase of interest.[12] Once the interferogram with modulated carrier fringes is recorded and analyzed, carrier is removed by subtracting the phase of the undeformed carrier fringes (SPUCF) from the recovered phase in the spatial domain. This method is particulary well suited for the analysis of fringe patterns in which the spatial carrier frequency is a function of the spatial coordinates, i.e., unequally spaced and/or twisted carrier fringes. Nevertheless, the use of an additional fringe pattern duplicates the number of direct and inverse Fourier transforms, and hence the computing time. Also, the need of an additional fringe pattern makes the system sensitive to environmental disturbances, negating the advantage of FTM over temporal phase measurement methods.

A phase algorithm without the influence of carrier has been recently demonstrated for a phase-stepping profilometry system.[13] It makes the procedure of phase unwrapping easier because wrappings and some other discontinuities caused by the carrier frequency are removed. However, its application to other evaluation techniques, e.g. Fourier analysis of TV holography fringe patterns, is not straightforward.

3. Analysis of computer-generated fringe patterns

The use of computer-generated fringe patterns allows exact determination of the difference between the retrieved and the desired phases, as the original phase distribution is known. For that reason we have simulated the fringe patterns following the method described in Ref. 14, which models the process of generating correlation fringe patterns for an out-of-plane TV holography (TVH) interferometer. The TVH fringe patterns have been obtained for a resolution of 512×512 pixels by subtracting a speckle interferogram from another one with a known phase difference. The average speckle size is 2 pixels.

Three different cases are considered: (a) the carrier frequency is an integer, (b) the carrier frequency is not an integer number, and (c) the carrier frequency varies continuously along the vertical direction. Two fringe patterns are generated for each case (Fig. 1), containing pure and modulated carrier fringes, respectively. The phase term that introduces modulation in the carrier fringes is a conical surface. These modulated carrier fringes represent the pattern that could be obtained from an out-of-plane TVH inteferometer in which the test object undergoes an out-of-plane conical deformation and the reference beam is properly tilted. Actual values of the carrier frequencies for the generated patterns are u=15, 15.4 and 14.5+i/512 for cases (a), (b) and (c), respectively, being i a variable index from 1 to 512 expressing the row number. The conical phase term that represents the modulation is the same for the three cases. Its circular base (radius 200 pixels) is placed at the center of the image and its height is $2\times 2\pi$ radians. Hence, the external frame of the fringe pattern is free of the desired information, as required by the LSF method.

Fringe analysis and carrier removal are schematically described in Fig. 2. Fringe patterns are Fourier transformed by means of a 2D-FFT algorithm in a PC-based image processor. Filtering is performed in the Fourier plane by multiplying the spectra by a function that yields 1 inside a circle and 0 otherwise. The frequency coordinates of the center of this circular domain are set to 15 and 0 for the horizontal and vertical components, respectively, and the radius to 7 pixels. Moreover, (-15,0) are the frequency components of the translation given to the filtered sidelobes of the three modulated fringe patterns when they are analyzed by the TSFO method. A least-squares fit over an area of the fringe pattern formed by lines 1-50, lines 463-512, columns 1-50 and columns 463-512 is used to calculate the plane that represents the carrier phase in the LSF method for the fringe patterns in Figs. 1(d) to 1(f).

4. Assessment of methods

We have only taken into account phase errors due to carrier removal because the aim of our paper is to quantitatively compare the accuracy of three carrier removal methods: TSFO, LSF and SPUCF. The influence of errors sources other than carrier removal, for example carrier frequency determination or spatial frequency bandwith, is the same for the three methods above and it is not considered here.

To assess the performance of the TSFO, LSF and SPUCF methods, several figures of merit have been used. Their descriptions and expressions are listed in Table 1, where $\varphi(i,j)$ represents the original phase and $\varphi'(i,j)$ the retrieved phase for a pixel placed at the ith row and the jth column of the image. Relevant information can be obtained from the modulus of the difference between the retrieved and original phase distributions. The mean and maximum values as well as the standard deviation of the absolute error are calculated. The parameter called fidelity quantifies how well details are preserved.[15] Additional insight can be gained by means of the relative mean absolute error, that measures the relative weight of the errors. Values close to 1 are desirable for fidelity and close to 0 for the rest of parameters. Actual values of the parameters mentioned above are shown in Table 2. TSFO, LSF and SPUCF methods were tested over three different couples of computed-simulated fringe patterns as explained in the previous section, resulting in 9 values for each parameter. In addition to the numerical values, plots of the phase errors along the central row of the phase maps are shown in Fig. 3. In agreement with the arguments given in Section 2, the phase yielded by TSFO contain linear errors when carrier frequency is non integer, Fig. 3(c). Linear errors also occur when the phase is calculated by LSF whichever the carrier frequency is, Figs. 3(b)-3(d). In this case these errors are caused by taking for calculation of the plane coefficients the pixels from the edge of the fringe pattern domain.

5. Application example

Transient deformations can be qualitatively studied with standard pulsed TV holography.[16] We have reported in a recent paper an improvement of a standard pulsed TV holography system, that enables quantitative measurements of transient bending waves to be performed.[17] Spatial carrier is introduced in the fringe patterns by means of a novel optical setup that separates and recombines the object beams from a twin-cavity diode-seeded Nd:YAG pulsed laser. The concerned reader will find a detailed description of the experimental setup, spatial carrier generation and fringe analysis in Ref. 17.

The aim of this section is to quantify the differences that arise due to carrier removal in real measurements of transient bending waves. Fig. 4(a) shows a correlation fringe pattern obtained by double-pulsed-subtraction TV holography[17] for a metal plate impact-excited with a piezoelectric translator. Vertical carrier fringes appear modulated by the deformation undergone by the plate ≈20 μs after mechanical excitation. Spatial carrier frequency is calculated from Fourier spectrum of the fringe pattern. Fringes are analized by FTM, resulting in a deformation plus carrier phase map, Fig. 4(b). LSF method performs a least-squares plane fit over an external frame devoid of modulation (described in Section 3). A 3-D plot of transient deformation after phase unwrapping and carrier removal by SPUCF is presented in Fig. 4(c). In contrast to computer-generated fringe patterns, exact value of transient deformation is unknown, so it is not possible to measure absolute errors due to carrier removal in the analysis of experimental fringes. Instead, differences between phase distributions obtained by two different carrier removal methods are calculated. The phase differences plotted at Figs. 5(a) and 5(b) stress two facts. Firstly, the use of different carrier removal methods in the analysis of experimental fringe patterns by FTM gives raise to significant differences in the recovered phase, and secondly, these differences are more relevant along the direction of the spatial carrier. Figures of merit listed in Table 1 are inappropriate to assess the accuracy of TSFO, LSF and SPUCF methods when applied to experimental fringes because absolute errors are unknown. A further approach to evaluate

the performance of those methods over real fringes is to calculate the deviation of the measurements, defined as:

$$d(i,j) = \varphi'_{\max}(i,j) - \varphi'_{\min}(i,j) \tag{1.a}$$

$$\varphi'_{\max}(i,j) = \max\{\varphi'_{TSFO}(i,j), \varphi'_{LSF}(i,j), \varphi'_{SPUCF}(i,j)\} \tag{1.b}$$

$$\varphi'_{\min}(i,j) = \min\{\varphi'_{TSFO}(i,j), \varphi'_{LSF}(i,j), \varphi'_{SPUCF}(i,j)\} \tag{1.c}$$

where $\varphi'_{TSFO}(i,j)$, $\varphi'_{LSF}(i,j)$ and $\varphi'_{SPUCF}(i,j)$ are the phases retrieved by TSFO, LSF and SPUCF carrier removal methods, respectively. The term $d(i,j)$ has the physical meaning of an upper limit for the difference between two measurements, whichever method is used for carrier removal. Actual values of maximum, minimum, mean and standard deviation of $d(i,j)$ are listed in Table 3, expressed in both radians and nanometers.

6. Discussion and Conclusions

Numerical data in Table 2 reveal that SPUCF is the carrier removal method that introduces less error in the phase distribution for the computer-generated fringes analized in this paper. In the studied example fidelity of the retrieved phase is allways greater than 99% when SPUCF is used. Furthermore, it yields the lowest values of $|e|_{ave}$, $\sigma_{|e|}$ and r for the three cases compared. SPUCF may be used in the analysis of both interferograms with or without an area devoid of phase information. We can conclude that SPUCF is the most accurate carrier removal method in Fourier fringe analysis, and must be used if possible, i.e., if the environmental disturbances between the recording of undeformed and modulated carrier fringes is neglectable.

It must be noticed that there exist particular cases in which the preceeding conclusions are not valid. For example, if the carrier frequency has to be calculated from an extended

spectrum TSFO is not accurate. Phase distributions with a linear term are another exception because in this case TSFO and SPUCF will not perform correctly.

The choice between TSFO and LSF in applications where SPUCF is unsuited must be done regarding to the particular spatial carrier. If the value of the carrier frequency is integer, TSFO exhibits better performance than LSF. However, this assumption will not be true in practice. For the general case of a non integer carrier frequency, TSFO introduces greater errors in the retrieved phase than LSF. This is due to the "picket fence" effect.[6] Nevertheless, if the carrier frequency varies continuously across the fringe pattern, TSFO is more accurate than LSF. This is so because the spectrum of a continuously varying carrier frequency is spreaded across the Fourier plane rather than concentrated in a discrete point, and then some of the spectrum energy is located on the sampled frequencies or near them. TSFO also advantages LSF in that the unwraping procedure is easier, especially for the case of high carrier frequencies, because wrappings and poles due to the spatial carrier are removed from the phase maps.[13]

The result of the present study can be sumarised as follows. Errors due to carrier removal must be taken into account when using FTM for phase evaluation in high precision measurement systems. SPUCF is the most accurate carrier removal method in Fourier fringe analysis. If the immunity to external disturbances is critical in the application, either TSFO or LSF must be used. The right choice between one method or another is determined by the particular carrier frequency that is encoded in the fringe patterns. LSF is only advisable when the frequency of the carrier fringes is constant and non integer.

Acknowledgments

The authors thank the support of the following institutions: Xunta de Galicia (XUGA 32101B95), Comisión Interministerial de Ciencia y Tecnología (TAP95-0805-E) and Universidade de Vigo. Part of this work was presented at the Applied Optics Divisional Conference of The Institute of Physics.[18]

References

1. M. Takeda, H. Ina, and S. Kobayashi, "Fourier-transform method of fringe-pattern analysis for computer-based topography and interferometry", *Journal of the Optical Society of America* **72,** 156-160 (1982).
2. M. Kujawinska, "Spatial phase measurement methods", in *Interferogram Analysis*, D. W. Robinson and G. T. Reid, Ed., pp.141-193, IOP Publishing Ltd., Bristol (1993).
3. K. A. Nugent, "Interferogram analysis using an accurate fully automatic algorithm", *Applied Optics* **24,** 3101-3105 (1985).
4. D. J. Bone, H.-A. Bachor, and J. Sandeman, "Fringe-pattern analysis using a 2-D Fourier transform", *Applied Optics* **25,** 1653-1660 (1986).
5. R. J. Green, J. G. Walker, and D. W. Robinson, "Investigation of the Fourier-transform method of fringe pattern analysis", *Optics and Lasers in Engineering* **8,** 29-44 (1988).
6. D. R. Burton and M. J. Lalor, " Managing some of the problems of Fourier fringe analysis", *Proc. SPIE* **1163,** 149-160 (1989).
7. M. Kujawinska and J. Wójciak, "High accuracy Fourier transform fringe pattern analysis", *Optics and Lasers in Engineering* **14,** 325-339 (1991).
8. X. Li, Z. Zhang, and X. Wu, "Investigation of the Fourier transform method in analysis of photo-carrier fringe patterns", *Proc. SPIE* **2544** 343-353 (1995).
9. G. Lai and T. Yatagai, "Use of the fast Fourier transform method for analyzing linear and equispaced Fizeau fringes", *Applied Optics* **33,** 5935-5940 (1994).
10. J. Gu and F. Chen, "Fast Fourier transform, iteration, and least-squares-fit demodulation image processing for analysis of single-carrier fringe pattern", *Journal of the Optical Society of America A* **12,** 2159-2164 (1995).
11. R. W. T. Preater and R. Swain, "Fourier transform fringe analysis of electronic speckle pattern interferometry fringes from high-speed rotating components", *Optical Engineering* **33,** 1271-1279 (1994).
12. J. M. Huntley and J. E. Field, "High resolution moire photography: application to dinamic stress analysis", *Optical Engineering* **28,** 926-933 (1989).

13. H.-J. Su, J.L. Li, and X.-Y. Su, "Phase algorithm without the influence of carrier frequency", *Optical Engineering* **36,** 1799-1805 (1997).
14. A. Dávila, G. H. Kaufmann, and D. Kerr, "Digital processing of ESPI addition fringes", in *Proc. 2nd. Int. Workshop on Automatic Processing of Fringe Patterns,* W. Jüptner and W. Osten, Ed., pp. 339-346, Akademie Verlag, Berlin (1993).
15. A. Dávila, G. H. Kaufmann, and D. Kerr, "Scale-space filter for smoothing electronic speckle pattern interferometry fringes", *Optical Engineering* **35,** 3549-3554 (1996).
16. A. Fernández, A. J. Moore, C. Pérez-López, A. F. Doval, and J. Blanco-García, "Study of transient deformations with pulsed TV holography: application to crack detection", *Applied Optics* **36,** 2058-2065 (1997).
17. A. Fernández, J. Blanco-García, A. F. Doval, J. Bugarín, B. V. Dorrío, C. López, J. M. Alén, M. Pérez-Amor, and J. L. Fernández, "Transient deformation measurement by double-pulsed-subtraction TV holography and the Fourier transform method", submitted to *Applied Optics*.
18. A. Fernández, G. H. Kaufmann, and A. F. Doval, "Comparison of carrier removal methods in Fourier transform fringe analysis", in *Proc. of the Appl. Opt. Div. Conf. of The Institute of Physics*, K. T. V. Grattan, Ed., pp. 11-16, Institute of Physics Publishing (1998).

Figure captions

Figure 1

Computer-generated fringe patterns: (a)-(c) Undeformed carrier fringes and (d)-(f) modulated carrier fringes. The simulated deformation is a conical surface. Carrier frequencies are: (a) and (d) 15, (b) and (e) 15.4 and (c) and (f) 14.5+*i*/512, where *i* denotes the row number.

Figure 2

Flow-chart of fringe analysis by FTM with three different methods of carrier removal: translation of the sidelobe to the frequency origin (TSFO), least-squares fit (LSF) and subtraction of the undeformed carrier fringes (SPUCF).

Figure 3

(a) 3-D plot of the computer-generated phase distribution. (b)-(d) Plots of the phase errors along the central row for the carrier frequencies: (b) 15, (c)15.4 and (d) 14.5+i/512.

Figure 4

Experimental results: (a) Correlation fringe pattern obtained by double-pulsed-subtraction TV holography ≈20 μs after a metal plate receives the impact of a piezoelectric translator. (b) Phase map, deformation plus carrier. (c) 3-D plot of transient deformation after phase unwrapping and carrier removal by SPUCF.

Figure 5

Experimental results. Differences between retrieved phases obtained by two different carrier removal methods: cross-section along (a) central row and (b) central column.

Table captions

Table 1

Figures of merit for a known phase distribution

Table 2

Numerical comparison of TSFO, LSF and SPUCF carrier removal methods for computer-generated fringe patterns with three different carrier frequencies.

Table 3

Figures of merit for an unknown phase distribution

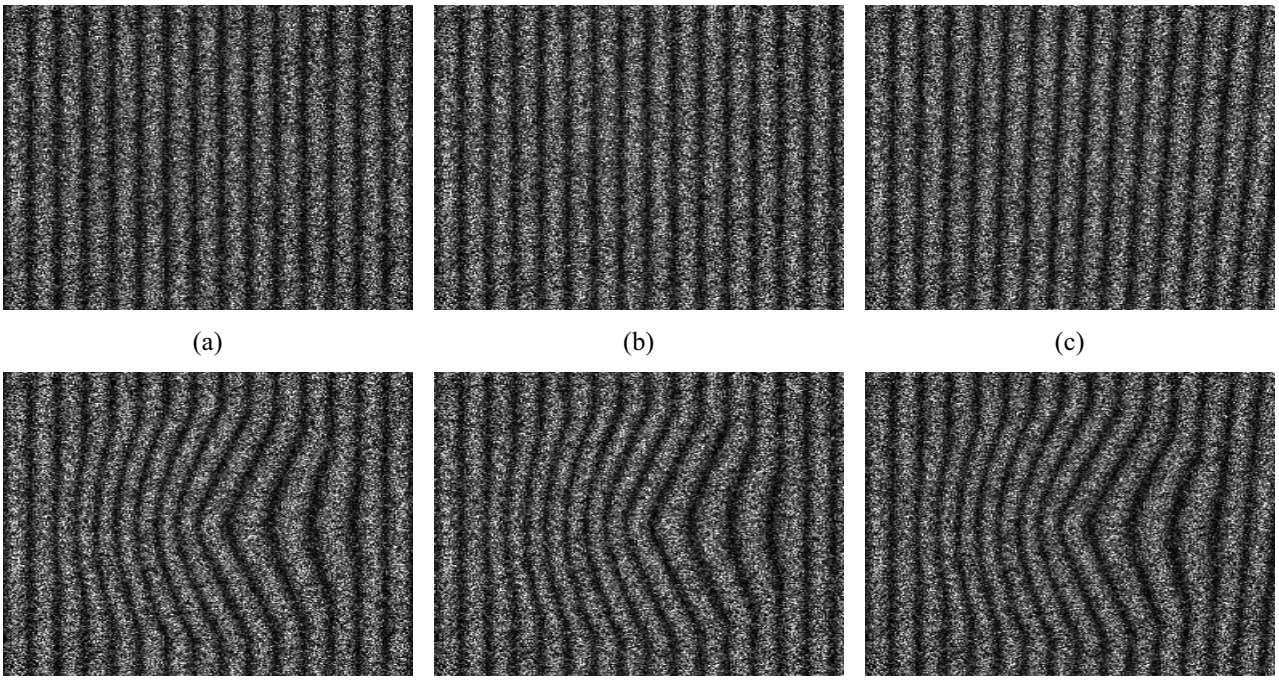

Figure 1
A. Fernández
Optical Engineering

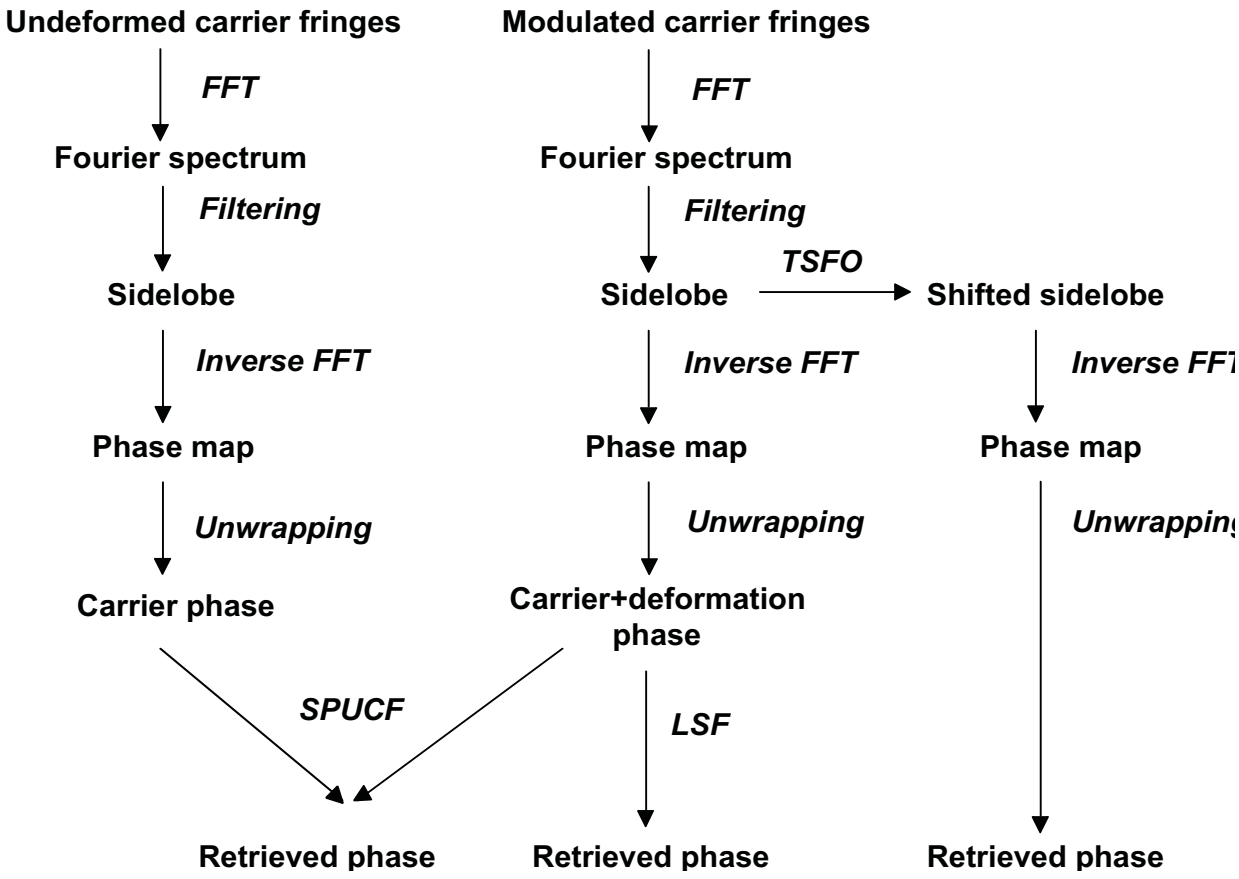

Figure 2
A. Fernández
Optical Engineering

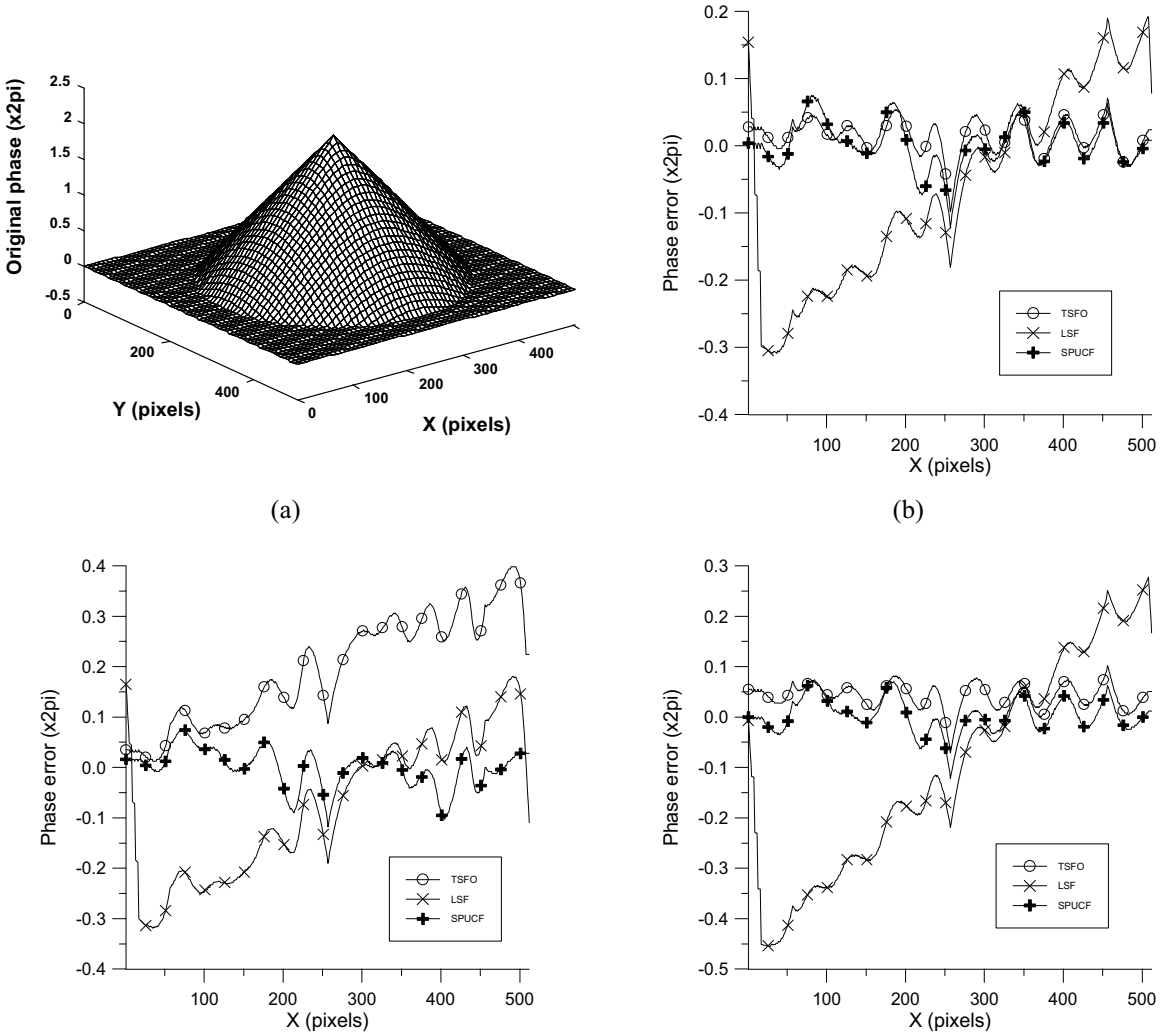

Figure 3
A. Fernández
Optical Engineering

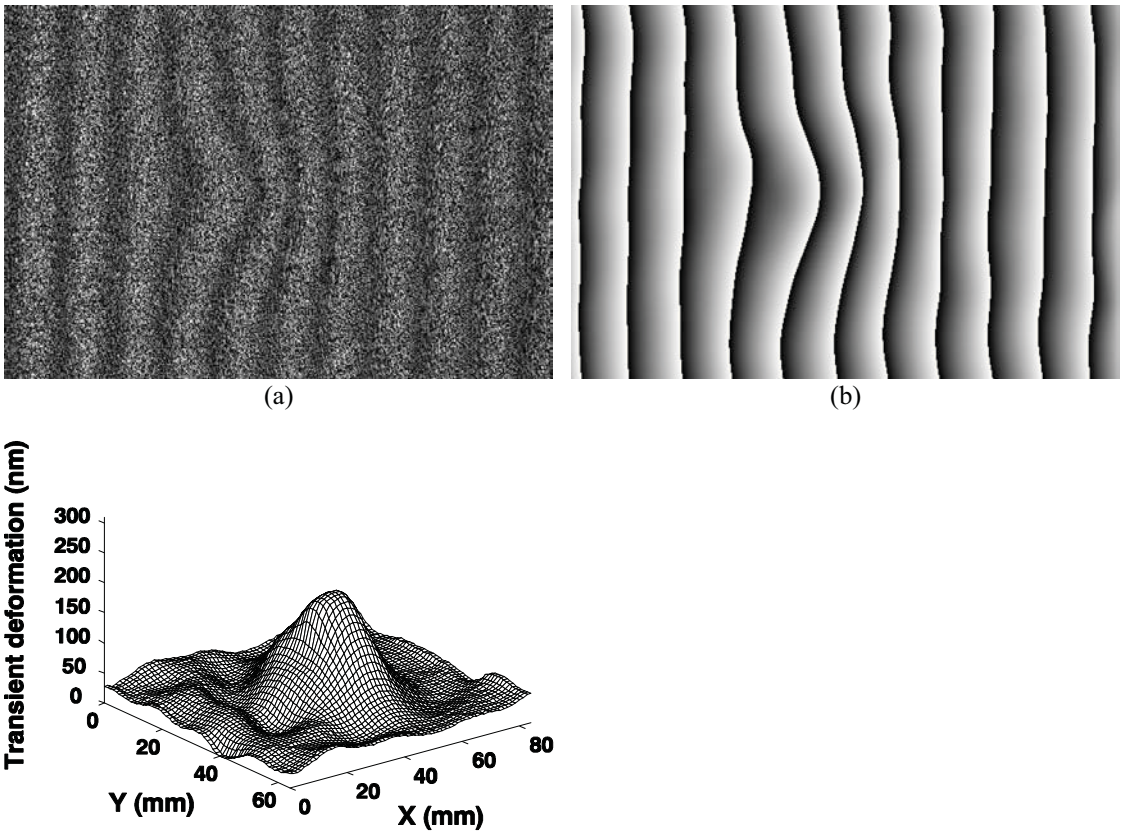

Figure 4
A. Fernández
Optical Engineering

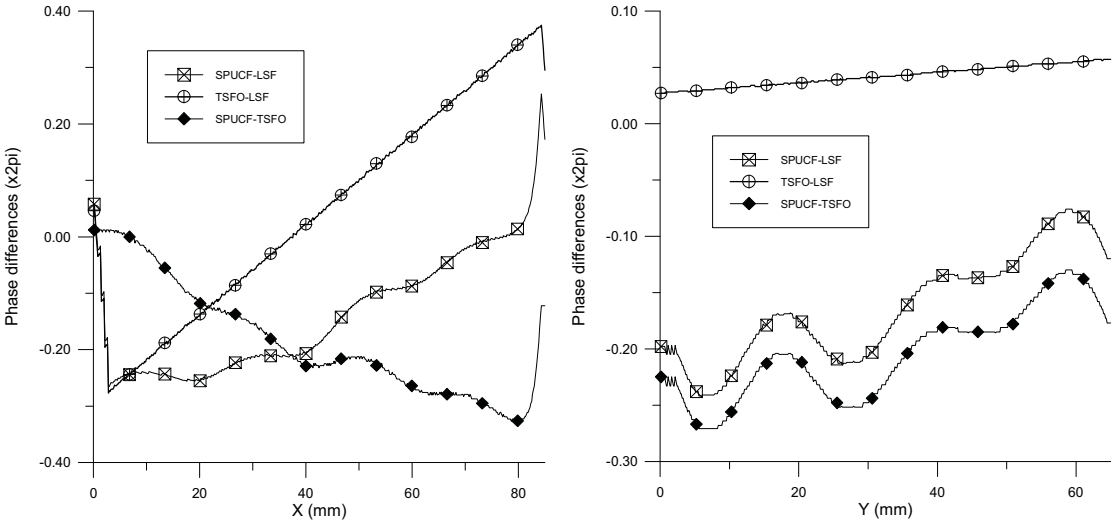

Figure 5
A. Fernández
Optical Engineering

Description	Expression
Mean absolute error	$\left\|e\right\|_{ave} = \dfrac{\sum_{i=1}^{512}\sum_{j=1}^{512}\left\|\varphi(i,j)-\varphi'(i,j)\right\|}{512\times 512}$
Standard deviation of the absolute error	$\sigma_{\|e\|} = \sqrt{\dfrac{\sum_{i=1}^{512}\sum_{j=1}^{512}\left[\left\|\varphi(i,j)-\varphi'(i,j)\right\|-\left\|e\right\|_{ave}\right]^2}{512\times 512-1}}$
Maximum absolute error	$\left\|e\right\|_{\max} = \max\left\{\left\|\varphi(i,j)-\varphi'(i,j)\right\|\right\}, 1\le i,j\le 512$
Fidelity	$f = 1-\dfrac{\sum_{i=1}^{512}\sum_{j=1}^{512}\left\|\varphi(i,j)-\varphi'(i,j)\right\|^2}{\sum_{i=1}^{512}\sum_{j=1}^{512}\varphi(i,j)^2}$
Relative mean absolute error	$r = \dfrac{1}{512\times 512}\dfrac{\sum_{i=1}^{512}\sum_{j=1}^{512}\left\|\varphi(i,j)-\varphi'(i,j)\right\|}{\sum_{i=1}^{512}\sum_{j=1}^{512}\varphi(i,j)}$

Table 1
A. Fernández
Optical Engineering

Carrier frequency	u=15			u=15.4			u=14.5+i/512		
Method	TSFO	LSF	SPUCF	TSFO	LSF	SPUCF	TSFO	LSF	SPUCF
$\lvert e\rvert_{ave}\ (\times 2\pi\ \mathrm{rad})$	0.02307	0.13849	0.01551	0.20798	0.13921	0.01716	0.13321	0.22277	0.01553
$\sigma_{\lvert e\rvert}\ (\times 2\pi\ \mathrm{rad})$	0.01690	0.09349	0.01546	0.11548	0.09666	0.01687	0.11061	0.14132	0.01594
$\lvert e\rvert_{max}\ (\times 2\pi\ \mathrm{rad})$	0.10630	0.41562	0.37402	0.46457	0.42430	0.34252	0.56693	0.73885	0.38189
f	0.99742	0.91203	0.99849	0.82170	0.90949	0.99818	0.90565	0.78074	0.99844
r ($\times 10^{-6}$)	0.2762	1.6579	0.1857	2.4898	1.6664	0.2054	1.5947	2.6668	0.1860

Table 2
A. Fernández
Optical Engineering

Parameter	Actual value (×2π rad)	Actual value (nm)
$d_{\max} = \max\{d(i,j)\}, 1 \le i, j \le 512$	0.4020	106.93
$d_{\min} = \min\{d(i,j)\}, 1 \le i, j \le 512$	0.0310	8.25
$d_{ave} = \dfrac{\sum_{i=1}^{512}\sum_{j=1}^{512} d(i,j)}{512 \times 512}, 1 \le i, j \le 512$	0.2471	65.72
$\sigma_d = \sqrt{\dfrac{\sum_{i=1}^{512}\sum_{j=1}^{512} (d(i,j) - d_{ave})^2}{512 \times 512 - 1}}, 1 \le i, j \le 512$	0.0665	17.68

Table 3
A. Fernández
Optical Engineering